# Computational Study of the Magnetocrystalline Anisotropy Energy of Ordered CoPt

Max Fusté Costa

October 2022

# Abstract

The study of the properties of magnetic materials is of primary importance in the development of new technologies. In this project, we aim to investigate the symmetries of some of the relevant properties of a cobalt and platinum alloy that emerge from the symmetry of the crystal structure of the alloy. More specifically, our goal is to calculate the magnetocrystalline anisotropy energy (MAE) for various orientations of the magnetization. The MAE is computed through the implementation of density functional theory (DFT) via the open-source package OpenMX.

The project consists of three main parts: Study on the convergence of the total energy of the system as a function of some relevant parameters, computation of the energy, the spin magnetic moment and the orbital magnetic moment as a function of the orientation of the magnetization, and a calculation of the magnetocrystalline anisotropy energy of the studied alloy.

The studied system is an ordered compound of cobalt and platinum, with a tetragonal crystal structure. The easy axis of magnetization was found to be along the c-axis of the crystal, and defined accordingly towards the z-axis in cartesian coordinates. The compound exhibits angular symmetry for the energy, the spin and orbital magnetic moments and the MAE, with a minimum energy along the easy axis of magnetization and a maximum at spherical angles $\theta$=90° and $\phi$=45°. Looking at the plots for the MAE, this maximum can be interpreted as an energy barrier that must be surpassed in order to invert the direction of the magnetization. Using an expression of the MAE in spherical angles, theoretical values for the anisotropy constants $K_1$, $K_2$ and $K_3$ are determined.

# Contents

# 1 Introduction

The last decades have seen the emergence of a new field inside of electronics that studies the intrinsic spin of the electron and its associated magnetic moment, known as spintronics. Progress in this field, which seemed only of academic concern at first, has supposed an increase in efficiency of data storage and transfer [1].

Magnetoresistive random access memory (MRAM) is an emerging technology that is a consequence of this progress. If the orientation of magnetization of a material can be regulated, it is then possible to store bits of information that can later be read by passing a current through the magnetized material. MRAM utilizes two magnetic layers separated by a thin insulating layer. The orientation of the magnetization of one of the layers with respect to the other dictates which bit is written (if the layers are oriented in the same way we have a 1, and if they are opposite to each other we have a 0) [2].

Magnets can lose or switch the orientation of their magnetization as a result of a small perturbation of the system. Magnetocrystalline anisotropy energy (MAE) measures how "hard" it is to magnetize a material in a particular direction over the necessary to magnetize it along its easy axis. This makes materials with a high MAE very useful for any type of magnetic recording or any other application of permanent magnets, thus being the study of this quantity in different materials of particular interest.

The aim of this project is to study the magnetic properties of a cobalt-platinum ordered alloy (CoPt). In particular, the magnetocrystalline anisotropy energy, which is expected to have an angular symmetry that emerges from the symmetry of the tetragonal crystal. This in turn motivates a study on the energy, the spin magnetic moment and the orbital magnetic moment.

The results were obtained from simulations performed using the open-source software OpenMX. OpenMX uses non-collinear density functional theory (DFT) to numerically solve the DFT equation, which is similar to the Schrösinger equation. Non-collinear DFT takes relativistic effects into account, including spin-orbit coupling (SOC), which are necessary to perform the calculations [3-6]. Solving the numerical problems is computationally heavy, requiring the use of powerful parallel computers. These computers were provided by Tetralith, a HPC cluster at NSC, which is a part of Linköping University (LiU) and the Swedish National Infraestructure for Computing (SNIC).

## 1.1 Crystal structure

A crystal is an ordered and periodic arrangement of atoms that extends in all three dimensions. The unit cell is the minimal structure of the crystal, reflecting its symmetry and structure. The repetition of this unit cells along the principal axes of the crystal defines the lattice. Mathematically, each axis can be defined by a translation vector, **a, b, c**. By traversing integer steps of the translation vectors, one can reach any lattice point from a given starting position. This can be expressed as $k\mathbf{a}+l\mathbf{b}+m\mathbf{c}$, where $k$, $l$ and $m$ are integers [7].

The material used in this study is an ordered alloy of cobalt (Co) and platinum (Pt). The crystalline structure of the so called $L1_0$ structure is tetragonal, which implies that all three translation vectors are perpendicular to one another, two being of the same length, different from the third [8]. By convention, the directions of the translation vectors are chosen to align with the x, y and z axes, and specifically the z-axis is chosen to be the one with different length. Additionally, for reference, the x-axis is defined in Figure 1 to be along the dashed line that is perpendicular to the plane of the paper. For the used alloy, the translation vectors have values of **a**=2.698 Å, **b**=2.698 Å, and **c**=3.727 Å. The volume of the unit cell can be calculated from these values by following equation.

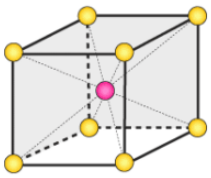

Figure 1: Crystal structure of ordered CoPt ($L1_0$). Here, the yellow spheres represent the cobalt and the pink one represents the platinum. The unit cell contains only one atom of cobalt and one atom of platinum.

$$V = abc = 27.13\mathring{A}^3 \tag{1}$$

## 1.2 Magnetocrystalline anisotropy energy (MAE)

Magnetocrystalline anisotropy is the dependence of the energy required to magnetize a material along a certain direction, relative to the crystal lattice. A magnetically anisotropic material often has two

preferred orientations of magnetization, corresponding to the lowest energy states. This direction is labelled as the easy axis of magnetization (and often related with the z-axis in cartesian coordinates). The MAE is the excess energy required to magnetize a material in a particular direction over the energy needed to magnetize it along the easy axis. If this value is sufficiently high, the direction of the magnetization will not spontaneously switch away from the easy one as a result of a perturbation of the system. Therefore, materials with high MAE are widely used as permanent magnets.

The MAE for a tetragonal crystal, as is the case of the alloy used in this study, is given by the following equation [9,10],

$$\frac{E}{V} = K_1 \sin^2(\theta) + K_2 \sin^4(\theta) + K_3 \sin^4(\theta)\cos(4\phi). \tag{2}$$

Here, the coefficients $K_1$, $K_2$ and $K_3$ are the so called anisotropy constants, which can be determined either computationally or experimentally [9-11]. The angles, $\theta$ and $\phi$, are the the ones from the spherical coordinate system. As the easy axis is aligned with the z-axis, $\theta$ can be defined as the angle from the easy axis toward the magnetization vector, and $\phi$ is the angle from the x-axis to the y-axis. For the purposes of this project, it will be interesting to consider the previous equation at leading order [9],

$$E = K \sin^2(\theta). \tag{3}$$

Given the high symmetry of the crystal structure, a symmetry of the MAE depending on the angles is expected. Calculating the MAE for two planes (which means fixing one angle while varying the other) should manifest this expected symmetry, which would also mean that a sampling of only two planes is sufficient to define the MAE in the entire space.

The expected symmetries of the MAE motivate a study on the relevant quantities that define the system (namely the energy, the spin magnetic moment and the orbital magnetic moment) and their behavior as $\theta$ and $\phi$ vary.

# 2 Method

This section gives an overview on the methods used to study the desired system and extract relevant information from it.

## 2.1 Density Functional Theory (DFT)

Density Functional Theory (DFT) is a computational method used to perform numerical simulations of quantum mechanical systems. In computational materials science, DFT is used to solve the Kohn-Sham equation, which is similar to the Schrödinger equation, to calculate the total energy of the system.

Consider a system of N electrons and M nuclei, at positions $\mathrm{r_i}$ and $\mathrm{R_j}$. This system can be fully described by the time-dependent Schrödinger equation [12], expressed as:

$$\begin{aligned}\hat{H}_{\mathrm{eN}} = &-\sum_{i=1}^{N} \frac{\hbar^2}{2m}\nabla^2_{\mathbf{r}_i} - \frac{1}{4\pi\epsilon_0}\sum_{i=1}^{N}\sum_{j=1}^{M}\frac{e^2 Z_j}{|\mathbf{r}_i - \mathbf{R}_j|} + \frac{1}{4\pi\epsilon_0}\sum_{i=1}^{N}\sum_{j=i+1}^{N}\frac{e^2}{|\mathbf{r}_i - \mathbf{r}_j|} \\ &-\sum_{i=1}^{M} \frac{\hbar^2}{2M_i}\nabla^2_{\mathbf{R}_i} + \frac{1}{4\pi\epsilon_0}\sum_{i=1}^{M}\sum_{j=i+1}^{M}\frac{e^2 Z_i Z_j}{|\mathbf{R}_i - \mathbf{R}_j|}.\end{aligned} \tag{4}$$

From left to right, the terms correspond to the kinetic energy of the electrons, the Coulomb interaction energy between electrons and nuclei, the Coulomb interaction energy between electrons, the kinetic energy of the nuclei and the Coulomb interaction energy between nuclei.

Since the nuclei are many times more massive than the electrons,the Born-Oppenheimer approximation can be used to simplify the Hamiltonian. This approximation considers the nuclei to be fixed in space, so the Hamiltonian describes only the electrons [12]. The previous equation can thus written as:

$$\hat{H}_{\mathrm{e}} = -\sum_{i=1}^{N} \frac{\hbar^2}{2m}\nabla^2_{\mathbf{r}_i} - \frac{1}{4\pi\epsilon_0}\sum_{i=1}^{N}\sum_{j=1}^{M}\frac{e^2 Z_j}{|\mathbf{r}_i - \mathbf{R}_j|} + \frac{1}{4\pi\epsilon_0}\sum_{i=1}^{N}\sum_{j=i+1}^{N}\frac{e^2}{|\mathbf{r}_i - \mathbf{r}_j|}. \tag{5}$$

The non-relativistic Schrödinger equation fails to capture magnetism, as spin angular momentum does not appear in this formulation. The most rigorous approach is to use the Dirac Hamiltonian, as it is fully relativistic.

A numerical resolution of this equation is not computationally plausible, given the sheer amount of memory required to even store the wave function obtained from solving a many-body quantum mechanical system. This problem can be solved by using DFT, which is able to quantify the ground state of the system by knowing the electron density. In this approach, the electron density can be easily discretized, but its computation still requires the wave function. This issue can be circumvented by using the Kohn-Sham equation, which uses non-interacting particles that generate the same density as an interacting system. To do so, it uses and effective external potential that accounts for all relevant coupling phenomena, including spin-orbit coupling (SOC) [12].

$$\hat{H}_{KS}\Phi(\mathbf{r}) = (-\frac{\hbar^2}{2m_e}\nabla^2 + V_{KS}(n(\mathbf{r}),\mathbf{r}))\Phi(\mathbf{r}) = E\Phi(\mathbf{r}) \tag{6}$$

In practice, an initial guess of the electron density is required to compute the Hamiltonian. The Kohn-Sham equation is then solved, giving a new electron density function. The problem is considered solved when the electron density function is sufficiently converged. The studied system requires SOC, which is not supported in collinear DFT. Fortunately, the program used to run the simulation, OpenMX, supports non-collinear DFT [3-6].

## 2.2 Convergence study

Before any physical study can be performed on the system, a convergence study is required. This study aims to ensure the reliability of the results by making sure that the simulation is sufficiently accurate. In order to estimate when the simulation is accurate, a study of the convergence of the total energy of the system is performed, as this quantity is of prime importance to both the later study and the description of the system.

The convergence study is performed in three steps in order to ensure the accuracy of the results. The first step uses different resolutions of the grid size while maintaining the value of the energy cut-off set to the default one. After the adequate size of the grid is determined, another study of the convergence of the same quantity is performed, now varying the energy cut-off value. Lastly, another run on the grid size is necessary to confirm the results.

### 2.2.1 K-grid

The first studied parameter is the k-grid, which refers to the discretization of the first Brillouin zone in the k-space (reciprocal). The parameter consists of three positive integers, one referring to the number of grid points in each direction. The length of a vector in the reciprocal lattice is inversely proportional to its normal counterpart. Additionally, it is necessary for the grid to maintain the size ratios between the three directions in order to keep the proper size of the first Brillouin zone. If we label the integers that represent each of the three directions as a, b, and c, with a ratio of a:b:c, we can estimate the size of the first Brillouin zone in the reciprocal space. In our study, the values of these parameters are as follows: a=2.698, b=2.698, c=3.727. The values of the reciprocal parameters, and therefore the ratios, are:

$$\frac{1}{a} : \frac{1}{b} : \frac{1}{c} = \frac{1}{2.698} : \frac{1}{2.698} : \frac{1}{3.727} \tag{7}$$

which is approximately equivalent to (4:4:3). During the convergence study, we increase the size of the grid by this amount.

To show the convergence of the total energy, it is to be assumed that the last value is converged. Then, all the data is offset so that the last value is 0 and two horizontal lines are plotted at $\pm 1$ mHa around the last point. The total energy is considered to have converged when its value falls between these two lines.

### 2.2.2 Energy cut-off

The second studied parameter during the convergence study is the energy cut-off, which is a value of the energy used to prevent singularities from appearing during calculations of Fourier transformations. In our study, we increase the value from 200 to 400 in steps of 25.

### 2.3 Determining the symmetries of the system and the MAE

OpenMX allows for a constriction on the orientation of the spin along a certain axis. By solving the problem described in section 2.1 with the spin constrained along evenly spaced orientations, the symmetries of the system can be calculated. Specifically, the study is performed by setting a value of $\phi$ and then calculating said quantities for values of $\theta$ from 0° to 90° degrees, in intervals of 5°. The values of $\phi$ are also taken from 0° to 90°, in intervals of 15°.

The MAE of a system in a particular direction can be calculated by subtracting the energy along the easy axis from the energy obtained in that particular direction. This means that the aforementioned study is also relevant in determining the MAE, and might help show the expected symmetry of this quantity.

## 3 Analysis of the results

### 3.1 Convergence study

The results of the convergence study are shown in figure 2. After the first step of the study, it is clear that all grid sizes except for the smallest one, (4 4 3), have converged. Computational time increases significantly with the grid size, so it is preferable to use the smallest possible value. Therefore, we choose a grid size of (8 8 6). The second step of the study gives various options for the value of the energy cut-off, as it converges at a cut-off energy of 300 Ha. Again, we want to choose the smallest possible value of the energy cut-off, so we take 300 Ha. The third and last step confirms the value for the energy cut-off chosen during the previous step of the convergence study.

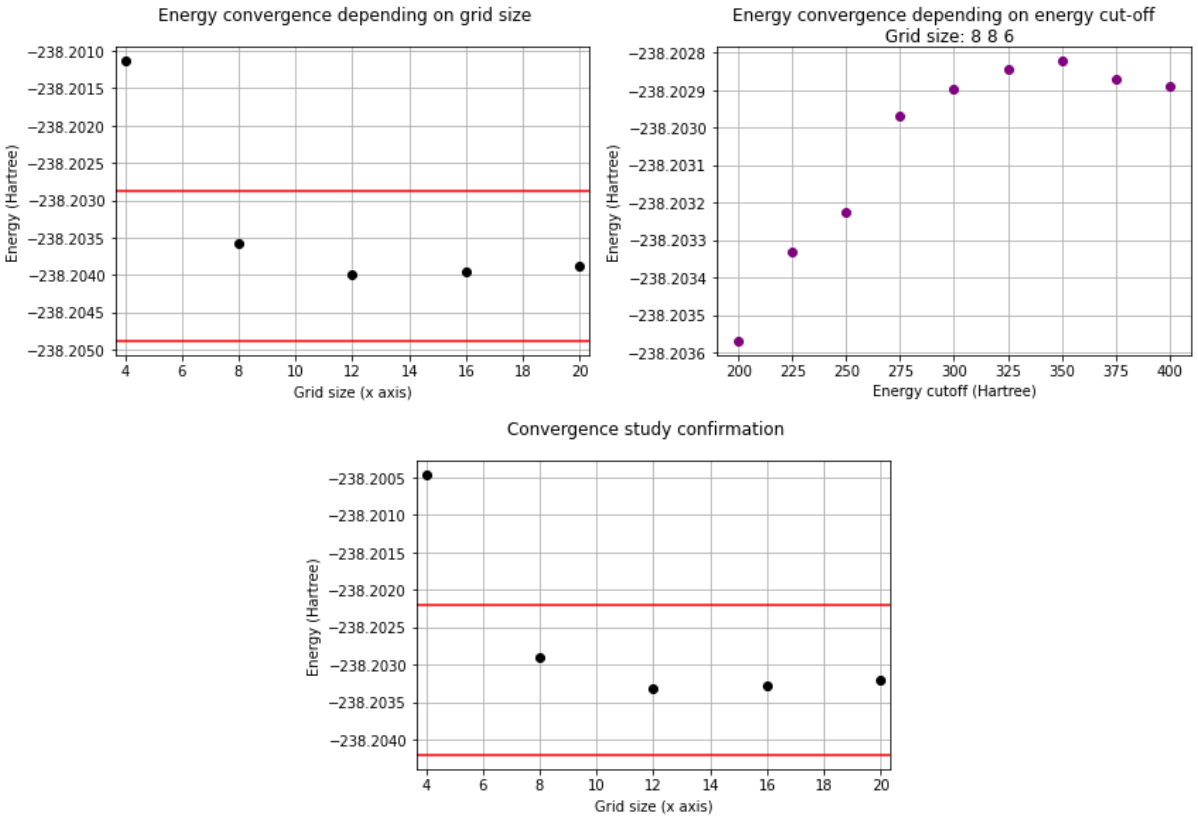


Figure 2: Convergence study. Left: Convergence of the total energy of the system as a function of the grid size. The points that fall between the two red lines (±1 mHa of the value of the last point, assumed converged) are considered to be converged. Centre: Convergence of the total energy of the system as a function of the energy cut-off with a set grid size of (8 8 6). Right: Confirmation of convergence study, equivalent to the first step, but with the energy cut-off obtained from the second one.

## 3.2 Symmetries

The result of the study on the symmetries of the system is shown in figure 3. The three observed quantities show a specular angular symmetry for both angles $\theta$ and $\phi$ centered on 45°. That is, for both the energy and the spin magnetic moment, the values increase with $\phi$ from 0° to 45°, and then decrease from 45° to 90°, mirroring the behavior from the first half of the values. The orbital magnetic moment shows a similar behavior, but with a minimum at 45°, instead of the maximum present on the other two quantities. For the spin magnetic moment the system shows a notable variation with both angles, with

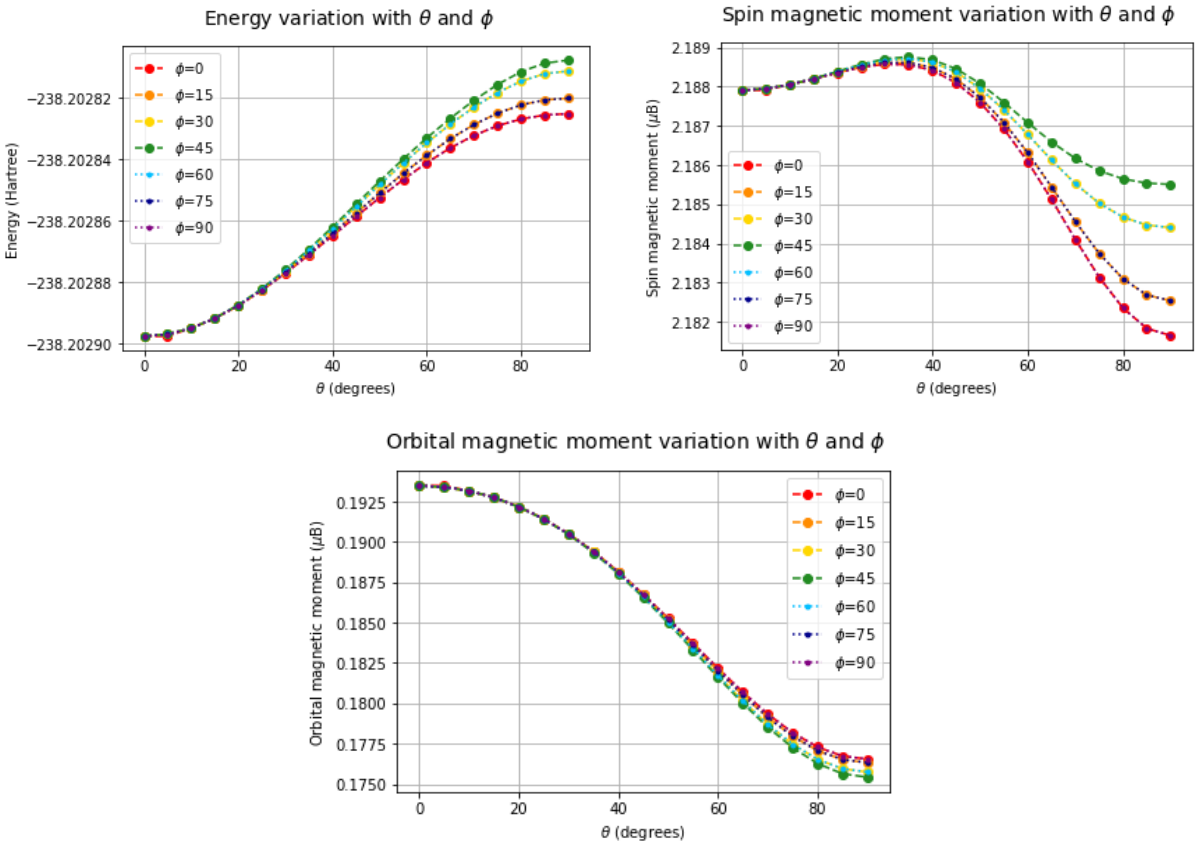


Figure 3: Calculated total energy, spin magnetic moment and orbital magnetic moment variation with the angles $\theta$ and $\phi$.

a maximum around the point where the system is the furthest away from $\theta$=$\phi$=0°. The energy and the orbital magnetic moment exhibit the same symmetry as the spin magnetic moment over $\phi$, even if less noticeably.

The magnetization depends on both the spin and orbital magnetic moments. It can be seen in figure 3 that the spin magnetic moment is around an order of magnitude larger than the orbital magnetic moment, and that the latter orients itself in approximately the same direction as the former. Thus, it can be stated that the direction of the magnetization is determined by the orientation of the spin magnetic moment. It is important to note that the the spin and orbital magnetic moments are varied along the same direction simultaneously.

### 3.2.1 Orbital and spin magnetic moment for cobalt and platinum

The individual contribution of cobalt and platinum to the orbital and spin magnetic moments is interesting, as it allows for an easier comprehension of the relevance of each element in the studied alloy for a given value of $\theta$ and $\phi$. As it can be seen by both comparing figures 3 and 4 and by checking the magnitude difference between both elements, it is clear that cobalt is the major contributor to both quantities. The contribution of platinum is of minor relevance for both the orbital and spin magnetic moment, even at their maximum values ($\theta$=90° for the orbital magnetic moment and around $\theta$=45° for the spin magnetic moment). Therefore, it must be added to the last statement of the previous section

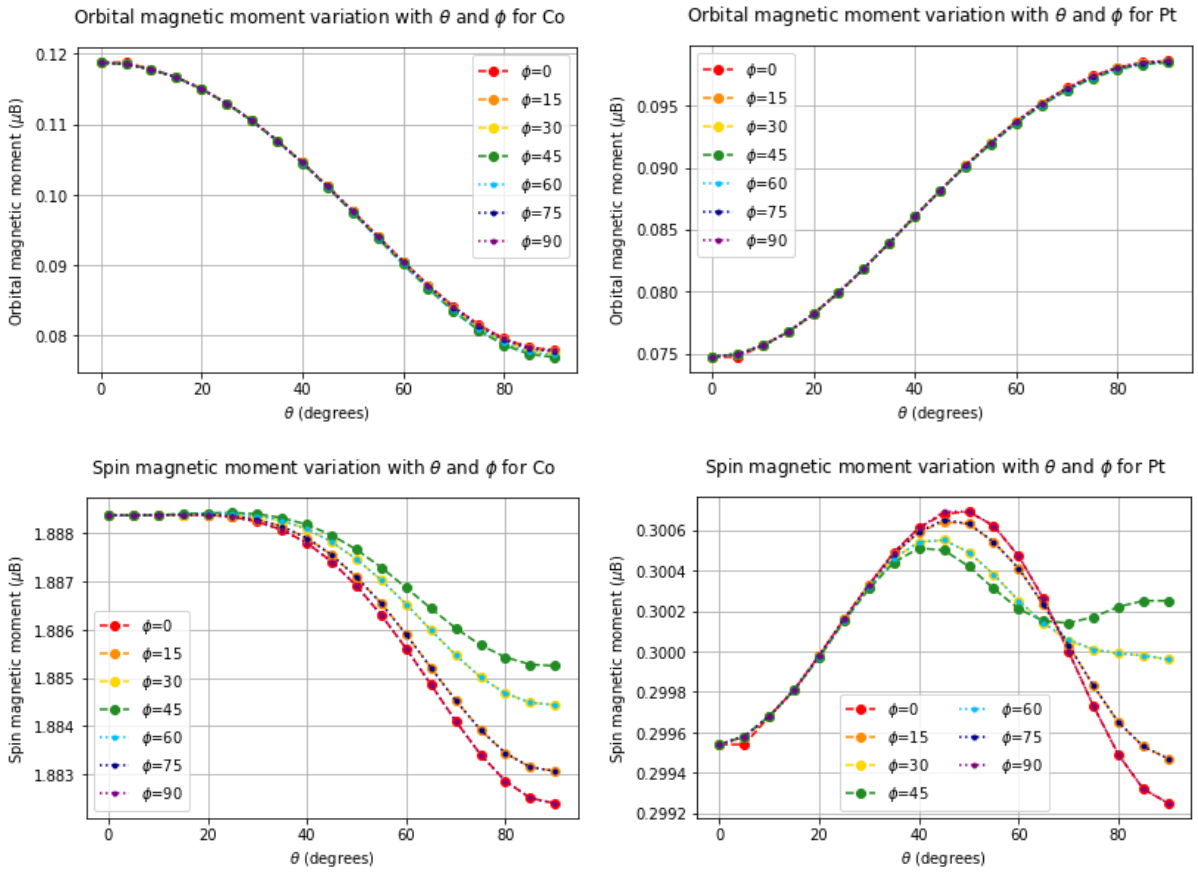


Figure 4: Orbital (top) and spin (bottom) magnetic moment separated for cobalt (left) and platinum (right) over the angles $\theta$ and $\phi$.

that not only is the orientation of the total magnetization determined by the spin magnetic moment, but that it is determined mostly by the spin magnetic moment of the cobalt.

### 3.3 Magnetocrystalline Anysotropy Energy (MAE)

Figure 5 shows the results of the MAE calculation. As expected, the system exhibits a symmetry over $\phi$, centered at 45°. What is perhaps more relevant is the right plot from this figure, which allows for a physical understanding of the consequences of this symmetry. Defining, as we have, the easy axis (or z-axis) as the one where $\theta$=$\phi$=0°, we see that in order to invert the direction of this axis, an energy barrier is to be crossed. The plot corroborates that this definition of the easy axis is correct, as it is where the energy is the lowest. Additionally, it gives an insight on the size of the barrier, this being of 0.4 meV/Co atom.

The results displayed on Figure 5 (left) exhibit maxima that vary from 0.002 to 0.0025 eV, depending on the angle $\phi$. These values are, respectively, of 11.81 and 14.76 MJ/$m^3$. Other studies have found values of similar magnitudes [8,13,14]. Specifically, Daalderop et al [13] non-self consistently computed a MAE of 2.0 meV per unit cell, whereas Oppeneer [14] computed the MAE self consistently and obtained 1.0 meV per CoPt cell.

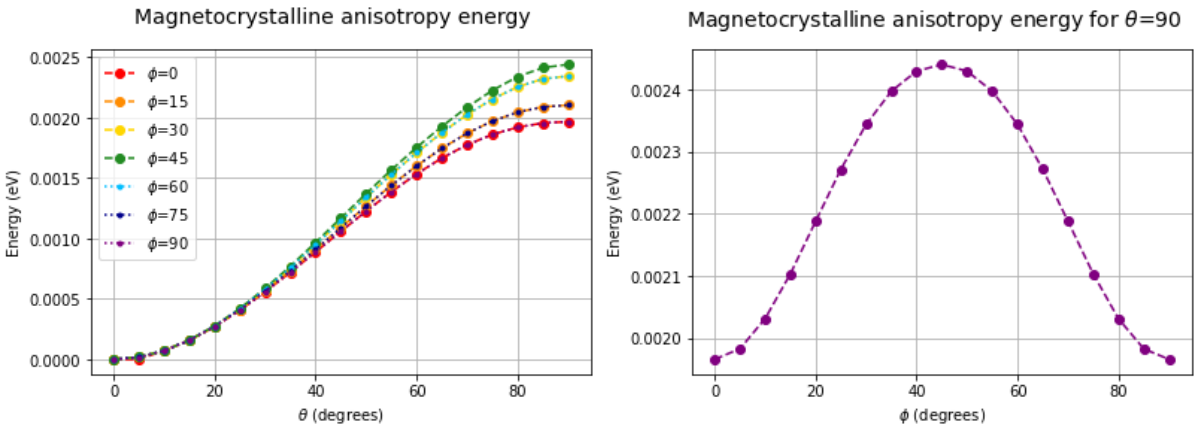


Figure 5: Left: MAE variation over the angles $\theta$ and $\phi$. Right: MAE variation over $\phi$ with a fixed value of $\theta$=90°.

### 3.3.1 Anisotropy constants

The anisotropy constants can be calculated from equation (2) [9-11]. By considering only the equation up to quadratic order, that is reducing it to equation (3), the first anisotropy constant can be calculated. The value of $K_1$ is the slope of the curve shown in Figure 6 (left) which plots the MAE per unit volume as a function of $\sin^2(\theta)$. The other plot in this same figure shows the variation of the constant with the angles $\theta$ and $\phi$. It is to be noted that the value of $K_1$ has a high dependency on $\phi$ as $\theta$ increases. This is caused by the nature of the approximation and so the value of $K_1$ must be taken as the one close to $\theta$=0° as possible. Therefore, we can consider $K_1$ to be roughly equal to 87.6 $\mu$eV/Å$^3$ (2.38 meV/unit cell).

The obtained value is significantly larger than the one obtained in previous experimental studies, that being of around 17.05 $\mu$eV/Å$^3$ [15]. The causes for this difference can be a result of either the purity of the sample, the size of the bulk or the temperature at which the experiment was performed.

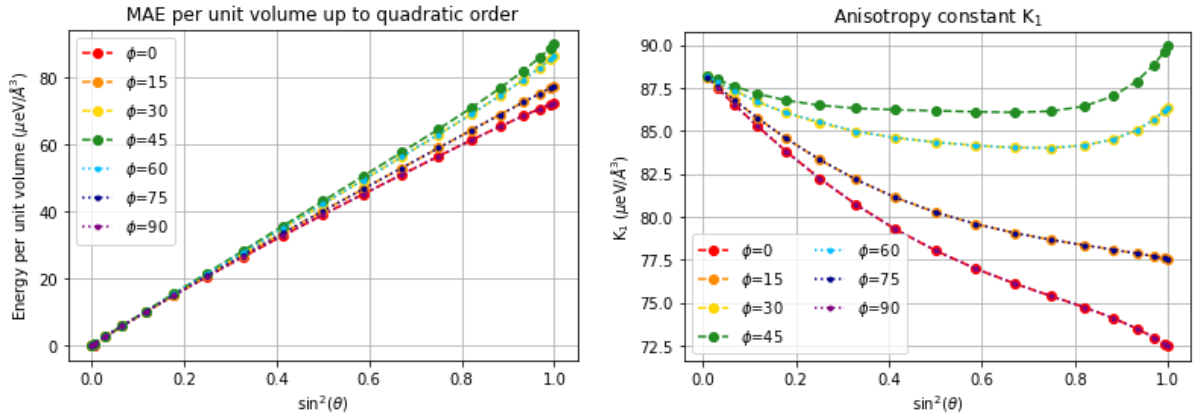


Figure 6: Left: MAE per unit volume up to quadratic order. Right: Value of the anisotropy constant $K_1$ as a function of the angles $\theta$ and $\phi$.

Next, we can calculate the third anisotropy constant, $K_3$. In order to do so, we must take $\theta$=90°, so that $\sin(\theta)$=1. This case is the one plotted in Figure 5 (right). $K_3$ can be calculated by taking the maximum and minimum values of the right plot of Figure 5 and calculating the semi-difference. The obtained value for $K_3$ is 8.73 $\mu$eV/Å$^3$ (0.237 meV/unit cell).

This same figure allows us to estimate the second anisotropy constant, $K_2$. By taking into consideration the equation that defines it:

$$\frac{E}{V} = K_1 + K_2 + K_3 \cos(4\phi), \tag{8}$$

we see that $K_1$+$K_2$ is a constant value that is not tied to any variable of the system. This allows us to

calculate it as the sum between the third anisotropy constant and the minimum value of the MAE for $\theta$=90°. $K_2$ is thus equal to -6.52 $\mu$eV/$\AA^3$ (-0.177 meV/unit cell).
Lastly, we can check the accuracy of the determined values for the three anisotropy constants by plotting the total energy per unit volume obtained by introducing the aforementioned values of $K_1$, $K_2$ and $K_3$ into equation (2) against the one obtained through the computation performed with OpenMX. The black continuous line in Figure 7 shows the ideal behavior of the plotted values if they where to be equal at every point, for every value of $\theta$ and $\phi$. However, even though this is true for small energies (which means small values of $\theta$), we can observe a deviation from the ideal behavior that can be due to the approximations taken into consideration for the calculation of the three anisotropy constants to avoid the apparent angular dependence. By taking the exact value of $K_1$ at every value of $\theta$ and $\phi$, as displayed in Figure 6 (right), we obtain a value for the total energy that adjusts better to the ideal behavior.

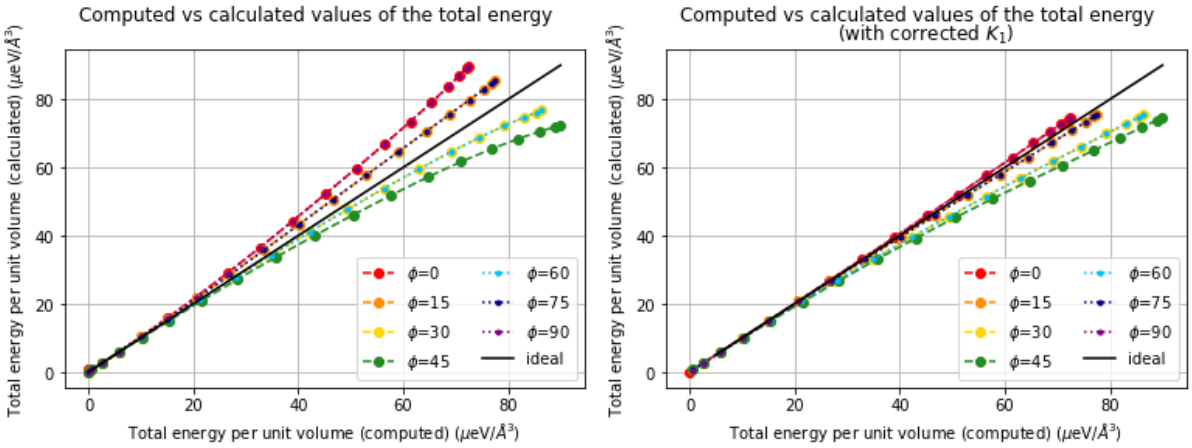


Figure 7: Comparison between the computed values of the total energy (obtained with OpenMX) and the calculated ones (obtained by introducing the values of $K_1$, $K_2$ and $K_3$ into equation (2). The plot on the right uses the values of $K_1$ displayed in Figure 6.

# 4 Conclusion

The study on the energy, the spin magnetic moment and the orbital magnetic moment confirmed the expected angular symmetry emerging from the crystal structure. It is of particular relevance the results extracted from the study of the energy, as the direction of the easy axis is confirmed to be the one pointing toward the c-axis of the tetragonal structure. This confirmation can also be extracted from the magnetocrystalline anistropy energy analysis.

The studies of both the spin and the orbital magnetic moments are of great interest, as they allow us to point out to Cobalt as the major contributor to these quantities and to the spin magnetic moment as the major contributor to the total magnetic moment, as was expected given the magnetic ordering of both components of the studied sample.

The magnetocrystalline anisotropy energy was found to be of the same order of magnitude (1-2 meV) as previous computational studies. The obtained results confirm the fact that the studied alloy is a good permanent magnet.

The study also found the values for the three anisotropy constants of lowest order. The first constant, $K_1$, was found to be 87.5 $\mu$eV/$\AA^3$, which is considerably greater than the one found in previous experimental studies. The causes for this difference can be a result of either the purity of the sample, the size of the bulk or the temperature at which the experiment was performed. The third anisotropy constant was found to be 8.73 $\mu$eV/$\AA^3$ and $K_2$ was found to be -6.52 $\mu$eV/$\AA^3$.

## Acknowledgements

This project was made possible by the efforts of both Peter Oppeneer and Leandro Salemi. Both of them have set aside incredible amounts of time from their busy schedules (and time from their summer vacation and weekends) to get this project going. I would also like to thank them to give me, a particle physicist, the opportunity to get a glimpse of the computational methods used in material science and, in particular, in the physics of magnetism, which have always been of great interest to me.

Fumiyuki Ishii, professor at Kanazawa University and one of the developers of OpenMX, in Japan, has also helped me a lot during this project. I want to thank him for his disponibility and interest in helping me with some of the problems I've faced while using OpenMX.

# References


[1] S. Bhatti et al. *Spintronics based random access memory: a review.* Materials Today, **20**, 530-548, 2017.

[2] B. Tudu and A. Tiwari. *Recent Developments in Perpendicular Magnetic Anisotropy Thin Films for Data Storage Applications.* Vacuum, **146**, 329-341, 2017.

[3] T. Ozaki. *Variationally optimized atomic orbitals for large-scale electronic structures.* Physical Review B. **67**, 155108, 2003.

[4] T. Ozaki and H. Kino. *Numerical atomic basis orbitals from H to Kr.* Physical Review B. **69**, 195113, 2004.

[5] T. Ozaki and H. Kino. *Efficient projector expansion for the* ab initio *LCAO method.* Physical Review B. **72**, 045121, 2005.

[6] K. Lejaeghere et al. *Reproducibility in density functional theory calculations of solids.* Science **351**, aad3000, 2016.

[7] C. Kittel. *Introduction to Solid State Physics*, 3rd ed. Barcelona, 3-4, 1993.

[8] P. Andreazza et al. *Structure and order in cobalt/platinum-type nanoalloys: from thin films to supported clusters.* Surface Science Reports **70**, 188-258, 2015.

[9] L.D. Landau, E.M. Lifshitz and L.P. Pitaevskii, *Electrodynamics of Continuous Media.* Course of Theoretical Physics, vol. **8**, 149-155, 2004 [First published in 1960].

[10] H. Shima et al. *Magnetocrystalline anisotropy energy in $L1_0$-type CoPt single crystals.* Journal of Magnetism and Magnetic Materials **290-291**, 566-569, 2005.

[11] K. Barmak et al. *On the relationship of magnetocrystalline anisotropy and stoichiometry in epitaxial $L1_0$ CoPt (001) and FePt (001) thin films.* Journal of Applied Physics, **98**, 033904, 2005.

[12] L. Salemi. *First-principles theory of electrically-induced spin and orbital magnetization*, Uppsala University, 22-31, 2022.

[13] G.H.O. Daalderop et al. *Magnetocrystalline anisotropy and orbital moments in transition-metal compounds*, Physical Review B, **44**, 12054, 1991.

[14] P.M. Oppeneer. *Magneto-optical spectroscopy in the valence-band energy regime: relation to the magnetocrystalline anisotropy.* Journal of Magnetism and Magnetic Materials, **188**, 275, 1998.

[15] R.A. McGurrie and P. Gaunt. *The magnetic anisotropy of ordered equiatomic platinum cobalt*, The Philosophical Magazine, **19**, 339-347, 1968.